

# Silicon Nanophotonics and Silicon-Organic Hybrid (SOH) Integration

*C. Koos<sup>1</sup>, L. Alloatti<sup>1</sup>, D. Korn<sup>1</sup>, R. Palmer<sup>1</sup>, T. Vallaitis<sup>1</sup>, R. Bonk<sup>1</sup>, D. Hillerkuss<sup>1</sup>, J. Li<sup>1</sup>, W. Bogaerts<sup>2</sup>, P. Dumon<sup>2</sup>, R. Baets<sup>2</sup>, M. L. Scimeca<sup>3</sup>, I. Biaggio<sup>3</sup>, A. Barklund<sup>4</sup>, R. Dinu<sup>4</sup>, J. Wieland<sup>4</sup>, M. Fournier<sup>5</sup>, J. Fedeli<sup>5</sup>, W. Freude<sup>1</sup>, and J. Leuthold<sup>1</sup>*

<sup>1</sup>Institute of Photonics and Quantum Electronics (IPQ) and Institute of Microstructure Technology (IMT), Karlsruhe Institute of Technology (KIT), 76131 Karlsruhe, Germany

Tel.: +49 721 608-42491, Fax: +49 721 608-42768, e-mail: christian.koos@kit.edu, web: www.ipq.kit.edu

<sup>2</sup> Photonics Research Group, Ghent University — IMEC, Dept. of Information Technology, B-9000 Gent, Belgium

<sup>3</sup> Department of Physics, Lehigh University, Bethlehem, PA 18015, USA

<sup>4</sup> GigOptix Inc., Switzerland and GigOptix Bothell (WA), USA

<sup>5</sup> CEA, LETI, Minatoc 17 rue des Martyrs, 38054 Grenoble, France

## Abstract

Silicon nanophotonics is considered a key enabler of future photonic-electronic information processing systems. Driven by substantial research investments, photonic integration on silicon-on-insulator (SOI) substrates has reached a degree of maturity that already permits industrial adoption. Silicon-organic hybrid integration (SOH) is a viable extension of the SOI material system for efficient electro-optic modulation and ultrafast all-optical signal processing.

## 1. Introduction

Data rates in information processing systems continue to grow exponentially, and the fundamental limitations of electrical interconnects in terms of bandwidth, spatial density and power consumption are becoming increasingly obvious [1], [2]. Short-reach chip and board-level optical interconnects could overcome these limitations, and highly scalable photonic device concepts and reliable integration techniques are currently subject to intense research efforts. Silicon nanophotonics is one of the most promising options featuring low fabrication costs, high integration density, and the potential for industrial mass production with mature CMOS technology [3]. For nonlinear-optical applications, the SOI material system can be extended by hybrid integration of silicon waveguides with organic materials [26].

In this paper, we give an overview on the current state of silicon nanophotonics and we report on recent progress in silicon-organic hybrid (SOH) integration. In Section 2, we review active, passive and nonlinear-optic device concepts that have been realized on silicon-on-insulator (SOI). The SOH technology platform is introduced in Section 3. In Sections 4 and 5, we discuss experimental demonstrations of electro-optic modulation at 42.7 Gbit/s and of all-optical signal processing at data rates of up to 170.8 Gbit/s.

## 2. Silicon nanophotonics

Over the last years, substantial research effort has been dedicated to nanophotonic integration on silicon-on-insulator (SOI) substrates. The current device portfolio comprises passive, active and nonlinear-optical components, and first silicon-photonic products are currently being commercialized. Most of these components rely on high index-contrast SOI strip waveguides with typical core heights of 220 nm and widths of less than 500 nm. While first waveguide generations suffered from roughness-induced scattering loss [4], continuous improvements of fabrication technology have reduced propagation losses to typical values of 1...3 dB/cm (0.17 dB/cm) for SOI strip (shallow-ridge) waveguides [5], [6]. Bend radii can be as small as 1  $\mu$ m without inducing appreciable radiation loss. The availability of compact low-loss waveguides has enabled a wide variety of passive devices such as, e.g., tunable add-drop multiplexers based on coupled ring resonators [7] or arrayed waveguide gratings [8].

Integration of active devices is hampered by the indirect band gap of silicon. All-silicon approaches to realize optical gain comprise, e.g., the use of stimulated Raman scattering [9] or the deployment of erbium-doped silicon nanocrystals [10]. Only recently, lasing has been demonstrated in tensile-strained n-doped germanium epitaxially grown on silicon [11] – a major step towards monolithic integration of electrically pumped lasers on silicon substrates. However, these approaches do not yet possess the degree of maturity needed for large-scale photonic-electronic integration. As an alternative, techniques for combining silicon with mature active III-V devices have been investigated. These techniques rely either on flip-chip integration and require careful alignment of III-V devices to pre-processed silicon waveguides [12], or on bonding of blank III-V dies to silicon substrates and subsequent collective processing on a wafer scale [13]. Using the latter approach, a wide variety of active devices on SOI has been demonstrated, comprising optical amplifiers, distributed-feedback (DFB) lasers, and even mode-locked lasers, see [14] and the references therein. Similar to light-emitting devices, silicon-based photodetectors for infrared telecommunication wavelengths can be realized by epitaxial growth of germanium on silicon [15] or by die-to-wafer bonding of III-V materials [16].

Electro-optic devices on silicon are currently based on free-carrier dispersion – silicon does not possess any appreciable second-order nonlinearities due to inversion symmetry of the crystal lattice. Using forward-biased pn-junctions integrated in nanophotonic rib waveguides,  $U_{\pi}L$  figures of merit of 0.36 V mm and modulation energies of 5 pJ/bit have been demonstrated, but bandwidths are limited by the slow recombination dynamics of the minority carriers [17]. Carrier depletion in reverse-biased pn-junctions can enable bandwidths of up to 30 GHz and data rates of

40 Gbit/s, but  $U_{\pi}L$  rises by about two orders of magnitude [18]. The performance of carrier-injection modulators is furthermore limited by the fact that the presence of free carriers changes both the refractive index and the absorption of the waveguide. Phase modulation is hence inevitably accompanied by amplitude fluctuations [19], and current SOI modulators are not well suited for use with complex quadrature-amplitude modulation (QAM) formats, where independent information is encoded on the phase and the amplitude of a signal.

Nanophotonic SOI waveguides seem to lend themselves for all-optical signal processing: Silicon possesses strong third-order nonlinearities, and nonlinear-optical interaction is enhanced by strong optical confinement [20]. However, Kerr-type cross-phase modulation and four-wave mixing can be significantly impaired by two-photon absorption (TPA) and TPA-induced free carrier absorption (FCA). Experimental demonstrations of all-optical signal processing in SOI waveguides comprise, e.g., signal regeneration at 10 Gbit/s [21] and demultiplexing from 1.28 Tbit/s to 10 Gbit/s [22]. For data rates of 40 Gbit/s, free carriers generated by TPA have to be removed by appropriate technological measures to prevent excessive absorption [23], which makes it difficult to achieve higher data rates.

Nevertheless, despite the deficiencies related to nonlinear-optic interaction in the SOI material system, first silicon photonic products are currently being commercialized. For example, California-based company Luxtera is offering a 40 Gbit/s active optical cable with integrated silicon-photonic transceiver chips. The cable supports 4 channels with data rates of 10 Gbit/s each. As optical sources, III-V laser diodes are directly attached to the SOI waveguides. Carrier-injection electro-optic modulators and Ge photodetectors are monolithically integrated together with electronics [24]. This is the first commercially available all-silicon photonic-electronic transceiver system.

### 3. Silicon-organic hybrid (SOH) integration

The silicon-on-insulator material system allows for high-density photonic-electronic integration on the basis of mature CMOS fabrication processes, but material properties are insufficient for some nonlinear optic applications such as efficient electro-optic modulation and impairment-free all-optical signal processing. In contrast to that, organic materials feature a low index contrast that does not permit dense integration, but provide a wide variety of optical properties that can be engineered by modifying the molecular composition. Silicon-organic hybrid (SOH) integration combines the advantages of both material systems: Nanophotonic SOI waveguides are embedded in organic cladding materials that provide the desired functionality [25], [26].

In an SOH device, the SOI waveguide cores must be designed such that interaction of the guided light with the cladding materials is enhanced. This can either be achieved by weakly guiding SOI waveguides with small core cross sections, or by using slot waveguide structures that consist of two silicon (Si) strips, Figure 1. For a quasi-TE mode, the dominant electric field component  $E_x$  is oriented horizontally. Electromagnetic boundary conditions require the horizontal component  $D_x$  of the dielectric displacement to be continuous across the core-cladding interface. The  $E_x$ -component hence features a discontinuity and the guided mode field is strongly confinement to the slot region [27], [20]. By using suitable functional cladding materials, the optical properties of the waveguide can be tailored to specific applications such as broadband electro-optic modulation [28] and all-optical signal processing that does not suffer from TPA-induced impairments [25], [29].

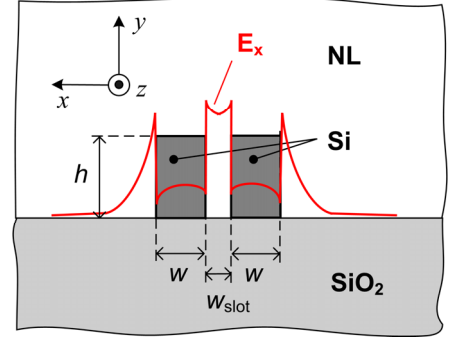


**Figure 1:** Cross section of an SOI slot waveguide consisting of two silicon (Si) strips on a silicon dioxide buffer layer ( $\text{SiO}_2$ ). The waveguide is covered by a nonlinear material (NL). For a quasi-TE mode, the magnitude of the dominant electric field component  $E_x$  is enhanced inside the slot.

### 4. SOH electro-optic modulators

A schematic view of an SOH slot waveguide modulator is depicted in Figure 2. Light is guided by two parallel silicon strips that are spaced by a narrow (typically 100 nm) gap. The silicon strips are electrically connected to metal transmission lines by thin conductive silicon slabs. A voltage applied to the transmission lines induces a strong electric field and a large electro-optic index change within the slot region where the optical mode field is concentrated. This structure has the potential to support data rates beyond 100 Gbit/s if appropriate measures are taken to increase the conductivity of the silicon slabs [26], [20].

For an experimental demonstration of electro-optic modulation in SOH waveguides, slot waveguide structures (240 nm strip width, 120 nm slot width) were realized within the European silicon photonics platform ePIXfab using DUV lithography and dry etching. The

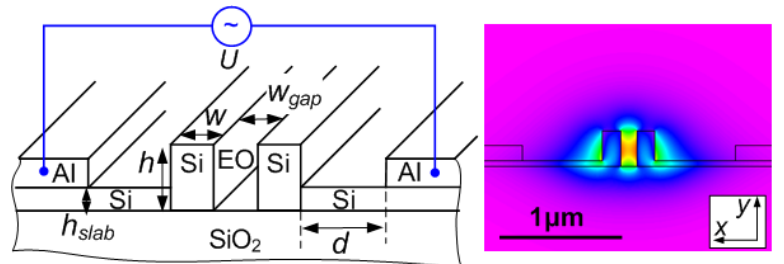


**Figure 2:** Slot waveguide SOH modulator concept: The silicon strips are electrically connected to metal transmission lines by conductive silicon slabs. The slot capacitance has to be charged via the resistive slab regions, and the bandwidth is limited by the corresponding RC time constant.

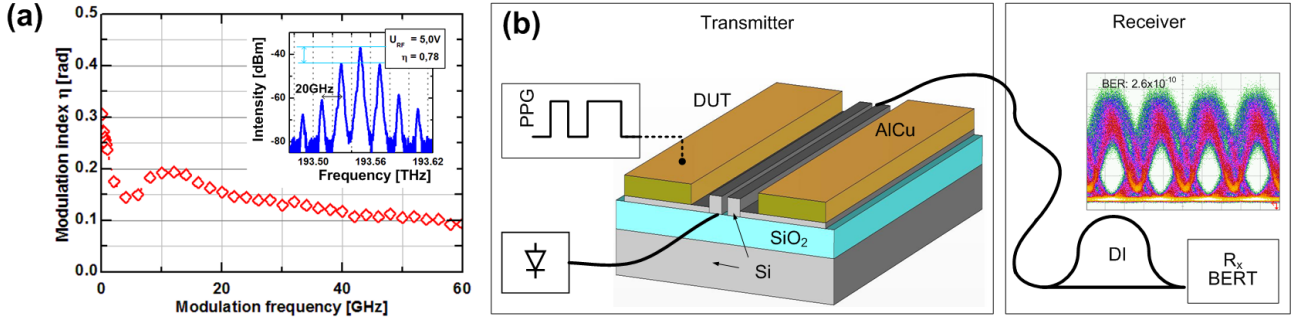


**Figure 3:** Experimental demonstration of electro-optic modulation in SOH waveguides. **(a)** Modulation index as a function of modulation frequency. The amplitude of the RF modulation signal is kept constant at 1 V. The inset shows the optical power spectrum of the phase-modulated optical signal at a modulation frequency of 20 GHz. **(b)** Data transmission experiment. Laser light is launched into the SOH slot waveguide, and an electrical 42.7 Gbit/s signal is fed to the electrodes. This generates a purely phase-modulated signal. On the receiver side, phase-to-amplitude conversion is achieved by feeding the signal into a delay interferometer (DI) that superimposes optical waves from subsequent bit slots. DUT = device under test, BERT = bit-error ratio tester.

structures were overlapped with an organic guest-host electro-optic material, which was poled by heating the sample above the material's glass transition temperature while applying a DC voltage to the slot waveguide. The waveguide was characterized by coupling an electrical radio frequency (RF) drive signal to the metal transmission lines. For sinusoidal modulation signals, the phase modulation index  $\eta$  was derived from the optical power spectrum. The frequency characteristic of the modulation index is plotted in Figure 3 (a). Above 2 GHz, the frequency response is essentially flat with a resonance peak at  $\sim 10$  GHz which is due to imperfect impedance matching of the  $50 \Omega$  transmission line. The frequency response of the device suggests that data rates well beyond 40 Gbit/s can be achieved [31]. In a transmission experiment, 1550 nm light was coupled to the waveguide and the modulator was driven with a 42.7 Gbit/s electrical signal (peak-to-peak amplitude of 4.1 V measured before the probe, PRBS length  $2^{31}-1$ ), Figure 3 (b). This produces a purely phase-modulated signal, which is detected using a one-bit delay interferometer at the receiver. Clear and open eye diagrams are found with bit error ratios as low as  $2.6 \times 10^{-10}$  [31]. The power consumption was estimated to be approximately 2 pJ/bit, and the data rate was only limited by the available pulse pattern generator, not by the device itself. This experiment represents the first demonstration of data encoding using an SOH electro-optic modulator. The device is a first-generation sample with significant potential for further improvement, but it can already compete with state-of-the-art carrier-injection phase modulators both in terms of power consumption [17] and bandwidth [18].

## 5. All-optical signal processing in SOH waveguides

For all-optical signal processing based on the Kerr effect, impairments induced by TPA-generated free carriers can be avoided when using SOH waveguides with third-order nonlinear cladding materials [25]. We fabricated different nonlinear silicon waveguides and measured the dynamics of cross-phase modulation using a heterodyne pump-probe technique [29]. Figure 4 depicts two different waveguide cross sections together with the respective pump-probe phase responses. For a conventional SOI strip waveguide operated in TE polarization, Figure 4 (a), the nonlinearity arises from the silicon core (Si-NL) and hence suffers from TPA. In the pump-probe phase response, this is clearly visible from a slow relaxation process caused by the presence of TPA-generated free carriers. Figure 4 (b) depicts an SOH slot waveguide. Optical nonlinearities originate from the nonlinear organic cladding (NL), and the phase response is ultra-fast without any appreciable impairment by TPA.

We experimentally demonstrated the viability of SOH slot waveguides in all-optical signal processing experiments [20]. Slot waveguide templates were again fabricated within the European silicon photonics platform ePIXfab using DUV lithography and dry etching [8]. The waveguide templates were functionalized by vapor deposition of a 950 nm thick amorphous organic film consisting of small organic molecules with a strong third-order nonlinear polarizability. The material is denoted as “derivative 2” in [32]. After deposition, cross-sectional profiles of the waveguides have been produced by focused ion beam (FIB) milling. The silicon strips exhibit a slightly trapezoidal

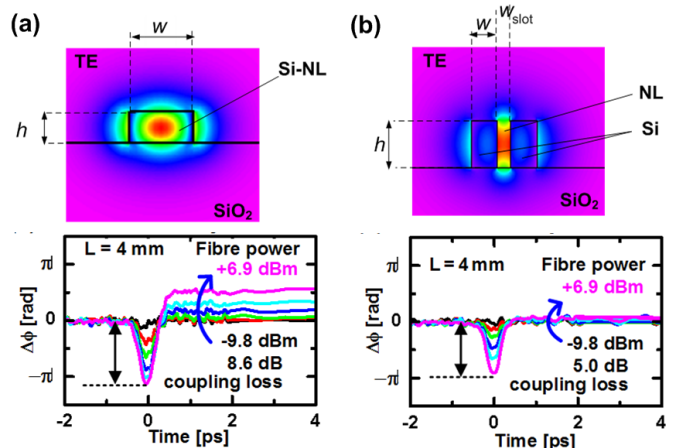


**Figure 4:** Electric field magnitudes (top) and pump-probe phase responses (bottom) of different waveguides. **(a)** Conventional SOI strip waveguide with a  $\text{SiO}_2$  cladding in quasi-TE operation. The phase-response exhibits a slow relaxation process caused by the presence of TPA-generated free carriers. **(b)** SOH slot waveguide in quasi-TE operation: Ultra-fast phase response, no TPA-generated free carriers [29].

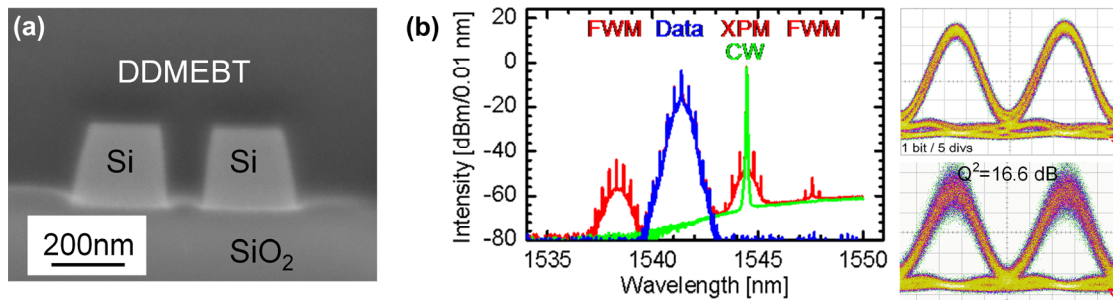


**Figure 5:** (a) Cross-sectional view of a fabricated silicon-organic hybrid (SOH) slot waveguide. (b) Wavelength conversion of a 42.7 Gbit/s data stream by cross-phase modulation (XPM) in an SOH slot waveguide: XPM spectra (left), input eye diagram (upper right) and received eye after XPM wavelength conversion (lower right).

shape, but the organic material homogeneously fills the slot without forming any voids, Figure 5 (a). Nonlinearity parameters of  $\gamma \approx 10^5 \text{ W}^{-1} \text{ km}^{-1}$  were measured. We demonstrated all-optical signal processing in Kerr-nonlinear SOH waveguides. Figure 5 (b) depicts wavelength conversion at 42.7 Gbit/s based on cross-phase modulation (XPM) [33]. Other experiments comprise wavelength conversion of a 56 Gbit/s quadrature phase-shift keying (QPSK) signal [34] and all-optical demultiplexing of signals with data rates of up to 170.8 Gbit/s [25].

## 6. Summary

Silicon photonics is an emerging technology which enables photonic-electronic integration based on mature CMOS fabrication. The basic building blocks for silicon photonic data transmission systems are available, and first commercial products are on the market. Silicon-organic hybrid integration (SOH) is a viable extension for silicon-based nonlinear optics that enables ultrafast all-optical signal processing and highly efficient electro-optic modulation.

This work was supported by the DFG Center for Functional Nanostructures (CFN), the KIT Initiative of Excellence, the Karlsruhe School of Optics and Photonics (KSOP), the EU-FP7 projects SOFI (grant 248609) and EURO-FOS (grant 224402), and by the BMBF joint project MISTRAL (German Ministry of Education and Research, grant 01BL0804). We are grateful for technological support by European silicon photonics platform ePIXfab.

## 7. References

- [1] [http://www.itrs.net/Links/2009ITRS/2009Chapters\\_2009Tables/2009\\_Interconnect.pdf](http://www.itrs.net/Links/2009ITRS/2009Chapters_2009Tables/2009_Interconnect.pdf)
- [2] Miller, D., *Proceedings of the IEEE* **97**(7), 1166 -1185 (2009).
- [3] Soref, R., *IEEE Journal of Selected Topics in Quantum Electronics*. **12**(6), 1678 -1687 (2006).
- [4] Poulton, C. G. *et al.*, *IEEE Journal of Selected Topics in Quantum Electronics* **12**(6), 1306 -1321 (2006).
- [5] Dumon, P *et al.*, *IEEE Photonics Technology Letters* **16**(5), 1328 -1330 (2004).
- [6] Dong, P. *et al.*, *Opt. Express* **18**(14), 14474-14479 (2010).
- [7] Popović, M. A. *et al.*, OFC 2008, paper OTuF4 (2008).
- [8] Bogaerts, W. *et al.*, *IEEE Journal of Selected Topics in Quantum Electronics*, **12**(6), 1394 -1401 (2006).
- [9] Rong, H. *et al.*, *Nature Photonics* **1**(4), 232-237 (2007).
- [10] Yuan, Z. *et al.*, *Proceedings of the IEEE* **97**(7), 1250 -1268 (2009).
- [11] Liu, J. *et al.*, *Optics Letters* **35**(5), 679-681 (2010).
- [12] Mitze, T. *et al.*, *Selected Topics in Quantum Electronics, IEEE Journal of* **12**(5), 983 -987 (2006).
- [13] Hattori, H. *et al.*, *IEEE Photonics Technology Letters* **18**(1), 223 -225 (2006).
- [14] Liang, D. & Bowers, J. E., *Nature Photonics* **4**(8), 511-517 (2010).
- [15] Michel, J.; Liu, J. & Kimerling, L. C. (2010), *Nature Photonics* **4**(8), 527--534.
- [16] Brouckaert, J.; Roelkens, G.; Van Thourhout, D. & Baets, R., *IEEE Photonics Technology Letters*. **19**(19), 1484-1486 (2007).
- [17] Green, W. M.; Rooks, M. J.; Sekaric, L. and Vlasov, Y. A., *Optics Express* **15**(25), 17106-17113 (2007).
- [18] Liao, L. *et al.*, *Electronics Letters* **43**(22) (2007).
- [19] Reed, G. T.; Mashanovich, G.; Gardes, F. Y. and Thomson, D. J. (2010), *Nature Photonics* **4**(8), 518-526.
- [20] Koos, C.; Jacome, L.; Poulton, C.; Leuthold, J. & Freude, W., *Optics Express* **15**(10), 5976-5990 (2007).
- [21] Salem, R. *et al.*, *Nature Photonics* **2**(1), 35-38 (2008).
- [22] Ji, H. *et al.*, *Journal of Lightwave Technology*, **29**(4), 426 -431 (2011).
- [23] Kuo, Y. H.; Rong, H. S.; Sih, V.; Xu, S. B.; Paniccia, M. & Cohen, O., *Optics Express* **14**(24), 11721-11726 (2006).
- [24] <http://www.luxtera.com/blazar-lux5010a.html>
- [25] Koos, C. *et al.*, *Nature Photonics* **3**(4), 216-219 (2009).
- [26] Leuthold, J. *et al.*, *Proc. IEEE* **97**(7), 1304-1316 (2009).
- [27] Almeida, V. R., Xu, Q., Barrios, C. A. & Lipson, M., *Optics Letters* **29**, 1209-1211 (2004).
- [28] C. Koos, J. Brosi, M. Waldow, W. Freude, and J. Leuthold, ECOC 2007, Paper P056.
- [29] Vallaitis, T. *et al.*, *Optics Express* **17**(20), 17357-17368 (2009).
- [30] Brosi, J.-M.; Koos, C.; Andreani, L. C.; Waldow, M.; Leuthold, J. & Freude, W., *Opt. Express* **16**(6), 4177-4191 (2008).
- [31] Alloatti L. *et al.*, Group IV Photonics 2010, China, paper ThC2 Sept. 2010
- [32] Michinobu, T. *et al.*, *Chemical Communications*, 737-739 (2005).
- [33] Vallaitis, T. *et al.*, *Intern. Conf. on Photonics in Switching (PS'09)*, Pisa, Italy, September 15-19, Postdeadline Paper PDP3 (2009)
- [34] Vallaitis, T. *et al.*, OFC 2010, paper OTuN1 (2010)